The potential use of gas hyperthermia in combination with radiofrequency plasma jet for the in vitro treatment of breast cancer

Jean-Sébastien Boisvert[1,2], Audrey Glory[1], Julie Lafontaine[1], Philip Wong[1,3] and Sylvain Coulombe[2]

[1]Institut du Cancer de Montréal, Centre de Recherche du Centre Hospitalier de l'Université de Montréal, 900 rue Saint-Denis, Montréal, Canada
[2] Plasma Processing Laboratory, Department of Chemical Engineering, McGill University, 3610 University Street, Montréal, Canada
[3] Département de Radio-oncologie, Centre Hospitalier de l'Université de Montréal, 1051 rue Sanguinet, Montréal, Canada

Abstract: A flowing capacitively-coupled radiofrequency (CCRF) discharge in helium is generated in a tubular coaxial configuration. The effect of direct exposure to the plasma effluents over a range of power levels on MDA-MB-231 breast cancer cells is investigated in the absence of culture medium. The plasma jet is found to kill the cancer cells with surface treatment being proportional to the plasma power. However, increasing the plasma power can lead to gas heating that potentially triggers thermal damage.

Keywords: Radiofrequency discharge, Atmospheric pressure, Plasma medicine, Cancer treatment.

1. Introduction

At atmospheric pressure, non-thermal plasma jets can be sustained with the help of field applicators of various geometries coupled to a myriad of voltage excitation waveforms [1]. One of the simplest configurations of plasma jets is the coaxial geometry, combined with a sinusoidal excitation waveform in the high-frequency range. In such conditions, the discharge sustained within the interelectrode region can be used to produce reactive species in the effluents. A possible application for those reactive species is cancer treatment [2]. In general, non-thermal plasma (NTP) sources used for oncology are required to be near room temperature (< 40°C) in order to completely avoid thermal damages of the treated tissues [3]. However, another physical therapy that has been used for cancer treatment, hyperthermia, takes advantage of thermal damage to cancer cells. In fact, throughout the years, different technics to locally apply hyperthermia have been developed. Ultrasound [4] and short wave [5] are good examples of such technologies. In this work, a preliminary *in vitro* study of the combination of hyperthermia (induced by gas) and NTP is undertaken.

2. Material and method

a. Discharge setup

The plasma jet is sustained by a flow of gas passing through electrodes in a coaxial configuration, separated by a dielectric material. The electrode configuration is shown in Fig. 1, where the ground electrode consists of a stainless steel tube (4 and 6 mm of inner and outer diameters, respectively) and the high-voltage electrode consists of a hollow stainless steel rode (0.686 and 1.067 mm of inner and outer diameters, respectively). A fused silica tube (3 and 4 mm of inner and outer diameters, respectively) act as the dielectric barrier ($\varepsilon_r = 3.75$) and covers the ground electrode. Experiments are performed by pulsing the gas flow with helium (99.999% purity) flowing at a maximum rate of 1 L/min and corresponds to a gas velocity of 70 cm/s. In this scheme, the power is turned on continuously, but the ignition of the discharge is controlled by the presence of helium flowing between the electrodes. The total discharge lasts about 2 s with a gas flow rate profile following a gaussian shape. Let us note that the high voltage electrode is hollow and enables the injection of a gas admixture at the exit of the device but is not utilized in this particular work [6].

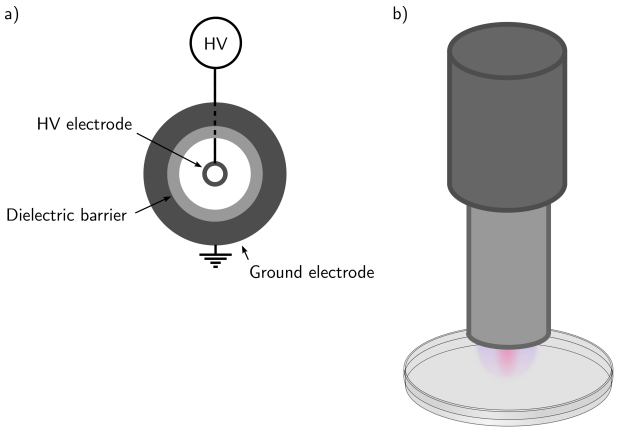

Fig. 1. a) Electrode configuration inside the field applicator and electrical circuit for high voltage supply and current/voltage measurements. b) Sketch of the plasma jet device during a treatment.

To investigate the behaviour of the discharge, optical diagnostics are performed. Pictures of the discharge are recorded with an Andor PCI iCCD camera (DH520-18F-01). The camera is positioned to collect the light coming from the discharge region between the electrodes. Optical emission spectra were also sampled in the electrode area and collected with the tip of an optical fibre (600 µm core diameter) pointing directly toward the plasma with the help of an Avantes AvaSpec-2048 spectrometer system (330 to 850 nm) equipped with a 2048 pixel CCD detector. Finally, temperature of the treatment is evaluated with the help of a thermocouple (Omega TJFT72-K) positioned at the same distance from the exit nozzle as the cells.

b. Cell culture and cytotoxicity essay

MDA-MB-231 triple-negative breast cancer (TNBC) cells were cultured in 24-well plates for 24 h to reach ~ 30 % confluence. The medium (Dulbecco's modified Eagle's medium (DMEM) supplemented with 10 % Fetal Bovine Serum) was withdrawn a few seconds before plasma treatment. Untreated fresh medium was added back onto the cells a few seconds after treatment (similar to the floating electrode DBD in [7]). Cytotoxicity was assessed by quantifying cellular Propidium Iodide (PI) stain uptake using live fluorescent microscopy at multiple time points after plasma treatment.

3. Results

a. Discharge behaviour

The nature of the discharge was investigated using the light distribution between the electrodes. Using the iCCD camera placed in front of the exit nozzle, the distribution of the light emission between the electrode is determined. This is shown in Fig 2.

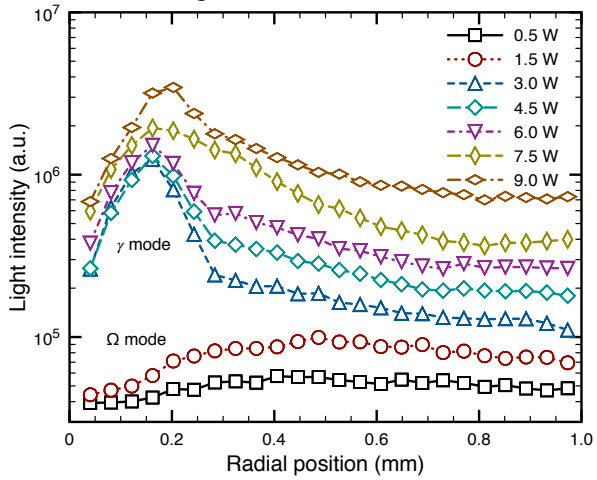

Fig 2. Profile of the light intensity (integrated from 180 to 850 nm) between the electrodes for different powers. The helium gas velocity is 70 cm/s at the exit and the camera integration time is 1 ms.

At low power, the spectrally integrated light emission is almost uniform across the gas gap with a small maximum at the centre of the gap. At higher power, the distribution of the light emission becomes highly non-uniform, with the maximum close to the high-voltage electrode. The behaviour of the light emission is typical of a CCRF discharge at atmospheric pressure with a gas gap of about 1 mm where the discharge is in either the Ω mode or the γ mode [8,9]. In the present situation, the fact that only one dielectric barrier is present between the electrodes (on the ground electrode) combined with the small radius of the high-voltage electrode (slight deviation from the uniform electric field produced by plane-to-plane configuration) makes the γ mode slightly non-uniform (exhibiting hot spots). These hot spots are expected from an atmospheric pressure CCRF discharge without a dielectric barrier on each electrode [10].

As the discharge is typical of atmospheric pressure radiofrequency discharges in the Ω and the γ modes, optical emission spectra are also quite similar to those presented in the literature for the same kind of discharge [11]. However, it is worth considering the influence of the power of some particular emission lines and bands. This is shown in Fig. 3 where the O($3^5P \rightarrow 3^5S$) (λ = 777.5 nm) and He($3^3S \rightarrow 2^3P$) (λ = 706.5 nm) atomic lines together with the $N_+^2(B^2\Sigma^+_u \rightarrow X^2\Sigma^+_g)$ (λ = 391 nm) and $N_2(C^3\Pi_u \rightarrow B^3\Pi_g)$ (λ = 357 nm) molecular bands are displayed.

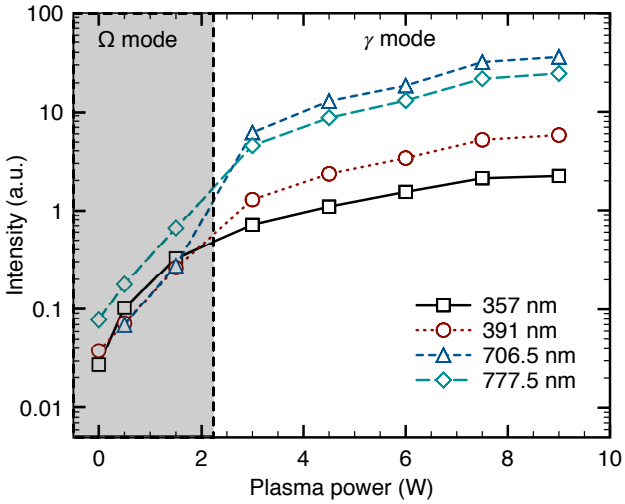

Fig. 3. Intensity of selected optical emissions as a function of the plasma power. The light is collected in the region between the electrodes and the optical system is corrected by its complete response curve.

It is observed that the helium only becomes the dominant emission when the discharge turns into the γ mode. This is coherent with the much higher electron energy reported in this discharge mode [12]. A consequence of the electron energy difference between the Ω and the γ mode is that the dominant chemical process can vary. As observed in Fig. 3, emissions associated with nitrogen and oxygen are dominant in the spectrum of the Ω mode, but not of the γ mode. This behaviour could have important consequences for the production of reactive oxygen and nitrogen species (RONS), that are known to play an important role in plasma medicine [13].

In order to determine the potential role of thermal damage to the cancer cells during the treatment with the plasma jet, the gas temperature of the effluent exiting the plasma jet nozzle was measured. This was done by placing the tip of the thermocouple 5 mm away from the exit nozzle, the same position where the cancer cells rest during their treatment. Time evolution of the thermocouple temperature, together with the maximum temperature during a gas pulse are shown in Fig. 4.

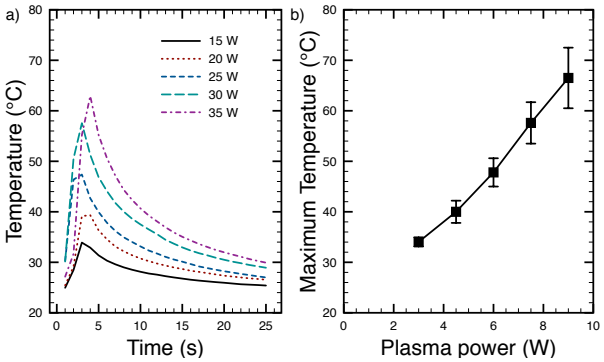

Fig. 4. a) Temperature evolution recorded by the thermocouple during the gas pulse 5 mm from the exit nozzle. b) Maximum temperature recorded by the thermocouple during a gas pulse. The error bar represents the standard deviation over multiple measurements.

During a gas pulse, the temperature of the thermocouple is found to rapidly reach a maximum after about 3 s following the beginning of its rise. Due to the latency of the thermocouple, the temperature decreases down to the room temperature in about 25 s or more. The maximum temperature during a gas pulse is found to increase linearly with the plasma power. While it is found to be potentially as high a 70 °C, in the Ω mode (as well as in the lower power branch of the γ mode), the temperature recorded by the thermocouple does not exceed 37 °C.

b. Treatment of breast cancer cells

Cytotoxicity of the treatment was measured using the death probe Propidium Iodide (PI) and live-cell fluorescence microscopy. Examples of image recorded within the treatment area are shown in Fig. 5.

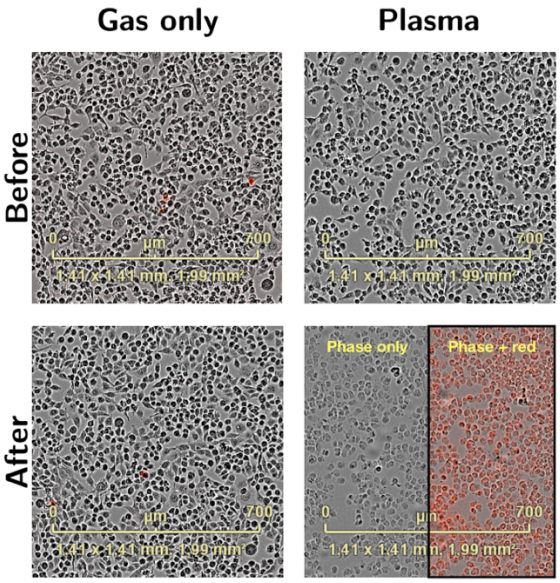

Fig. 5. Examples of fluorescence microscopy images (sub-images of the analyzed area) with (9 W) and without (0 W - gas control) plasma treatment, recorded about 3 h after the plasma treatment. Superposition of the phase and the red images unless otherwise stated.

First, even in the absence of cell culture medium over the cells, no morphological change or PI staining is observed in the case of the gas flow alone. This is remaining true as long as the gas flow and the treatment duration remain low (below ~ 70 cm/s and 2 s). Then, in the case of the plasma treatment, the "phase only" image shows that the cells are neither destroyed nor ablated. However, they are slightly contracted, and the cell membrane is likely damaged. As shown by the combination of phase and red image, the PI uptake is major after plasma treatment. In fact, every cell under the treatment area is found to exhibit a PI uptake, suggesting 100 % cell death within the treatment area.

While in Fig. 5, it is clear that every cell under the treatment area is affected by the plasma jet, the treatment area does not necessarily cover the entire well after a 2 s plasma pulse. To illustrate the extent of the treatment area, Fig. 6 shows a larger region of the well.

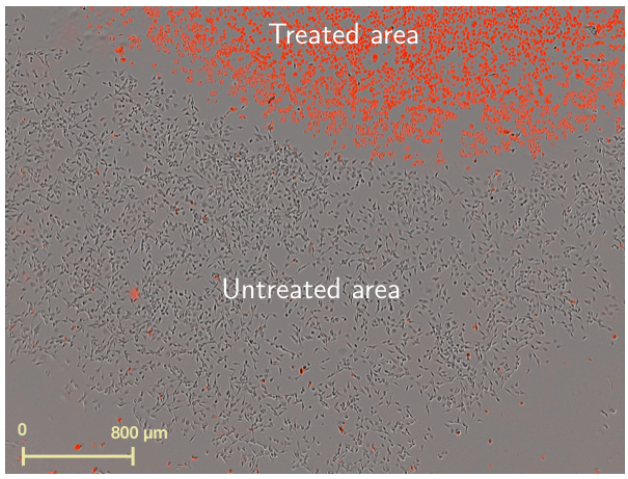

Fig. 6. Example of fluorescence microscopy image (sub-images of the analyzed area) recorded about 3 h after the plasma treatment at 9 W.

From Fig. 6, it is possible to observe that the treatment area can span over 1 mm radius (larger than the dimension of the area defined by the electrodes). It is also possible to see that the treatment is circumscribed within a very well-defined area and few PI uptake is recorded outside of this region.

To determine the effect of the plasma power on the efficacy of the treatment, the ratio of cells marked with PI over the total cell area was determined. This is shown in Fig. 7, where the number of red cells over the total area of cells clearly increases with the plasma power. Since 100 % of the cells in the area under the nozzle are marked with PI, this increase is due to an increase of radius of affected cells. However, as indicated by Fig. 4, the temperature of the gas can become significant in the γ mode. To evaluate the temperature at which thermal damage becomes important, the cumulative number of equivalent minutes at 43°C (CEM 43°C) is calculated for the 2 s gas pulse. As thermal damage to cells exposed to

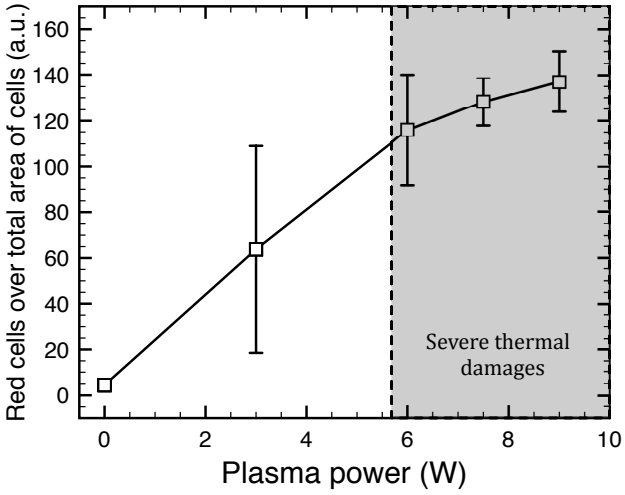

Fig. 7. PI positive cell number over total cell area (in the complete analyzed area) as a function of the plasma power during a gas pulse. Error bars represent standard deviation over n = 3.

temperature below 60°C is approximately linearly dependent upon exposure time and exponentially dependent upon the temperature elevation, CEM 43°C is a very effective tool to compare damage due to different hyperthermia modalities [14]. The CEM 43°C for the 2 s exposure is displayed in Fig. 8.

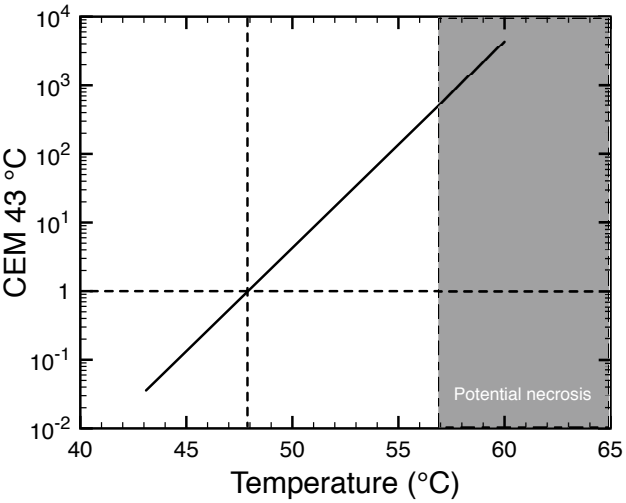

Fig. 8. CEM 43°C calculated for the temperature of 2 s plasma pulses [15].

Fig. 8 shows that 2 s of plasma exposure at 48°C is equivalent to 1 min of exposition at 43°C. Knowing that typical thermal necrosis occurs at about > 700 CEM 43°C [15], this is equivalent to > 57 °C of plasma exposure. Consequently, according to Fig. 4, thermal damage should be completely avoided in the Ω mode, but thermal necrosis could occur in the higher branch of the γ mode.

4. Conclusion

Controlled by the applied power, the discharge is found to be either sustained in the Ω and the γ mode. Both the Ω and the γ modes can be used to kill breast cancer cells. In the γ mode, the cytotoxic effect could be a combination of both hyperthermia and plasma. On the other hand, in the Ω mode the cytotoxic effect should be due to the plasma alone. In the future, the setup will be modified to enable the injection of preheated helium. This will allow to compare the plasma jet treatment with a gas-induced hyperthermia. Intracellular RONS levels are also under investigation.

5. Acknowledgements

The authors would like to acknowledge MEDTEQ, MITACS and NexPlasmaGen Inc. for their financial support. Special thanks to Professor Joëlle Margot for material contribution (iCCD camera).

6. References

[1] Winter, J., Brandenburg, R., and Weltmann, K.-D, Plasma Sources Science and Technology, 24 (6), (2015).
[2] Schlegel, J., Köritzer, J., and Boxhammer, V., Clinical Plasma Medicine, 1 (2), (2013).
[3] Dai, X., Bazaka, K., Richard, D. J., Thompson, E. R. W., and Ostrikov, K. K., Trends in biotechnology, (2018).
[4] Billard, B., Hynynen, K., and Roemer, R., Ultrasound in medicine & biology, 16 (4), (1990).
[5] Raoof, M., Cisneros, B. T., Corr, S. J., Palalon, F., Curley, S. A., and Koshkina, N.V., PloS one, 8 (7), (2013).
[6] Leveille, V. and Coulombe, S., Plasma Sources Science and Technology, 14 (3), (2005).
[7] Bekeschus, S., Lin, A., Fridman, A., Wende, K., Weltmann, K.-D., and Miller, V., Plasma Chemistry and Plasma Processing, 38 (1), (2018).
[8] Shi, J. and Kong, M. G., Journal of applied physics, 97, (2004).
[9] Boisvert, J.-S., Margot, J., and Massines, F., Plasma Sources Science and Technology, 26 (3), (2017).
[10] Shi, J., Liu, D., and Kong, M. G., Applied physics letters, 89 (8), (2006).
[11] Boisvert, J.-S., Vidal, F., and Margot, J., Physics of Plasmas (1994-present), 25 (8), (2018).
[12] Boisvert, J.-S., Montpetit, F., Margot, J., Vidal, F., and Stafford, L., Applied Physics Letters, (Accepted manuscript).
[13] Graves, D. B., Physics of Plasmas, 21 (8), (2014).
[14] Diederich, C. J, International journal of hyperthermia, 21 (8), (2005).
[15] Dewhirst, M. W., Viglianti, B., Lora-Michiels, M., Hanson, M., and Hoopes, P., International journal of hyperthermia, 19 (3), (2003).